Monthly Notices
of the
ROYAL ASTRONOMICAL SOCIETY

Mon. Not. R. Astron. Soc. **403,** 755–759 (2010) doi:10.1111/j.1365-2966.2009.16063.x

Evidence for an accretion steam in the low-accretion-rate polar J2048

S. Kafka,[1]★† C. Tappert[2]‡ and R. K. Honeycutt[3]

[1]*Spitzer Science Center/Caltech, MC 220-6, 1200 E.California Blvd, Pasadena, CA 91125, USA*
[2]*Departamento de Astronomia y Astrofisica, Pontificia Universidad Catolica, Vicuna Mackenna 4860, 782-0436 Macul, Chile*
[3]*Indiana University, Astronomy Department, Swain Hall West, Bloomington, IN 47405, USA*

Accepted 2009 November 17. Received 2009 November 9; in original form 2009 May 20

ABSTRACT

We present new red/near-infrared spectra of the low-accretion-rate polar J204827.9+005008.9. Compared to 2004 spectra in the literature, our 2008 data show more structured emission-line profiles. All emission lines in our spectra have two components at most orbital phases. The stronger component has a sinusoidal velocity variation ($K \sim 120$ km s^{-1}) and is likely due to irradiation of the inner hemisphere of the secondary star by the white dwarf. Based on the appearance of the Hα Doppler tomogram, the weaker, larger amplitude, line component likely originates in a ballistic stream from the L1 point. J2048 is thought to be accreting via a wind from the secondary star, so the detection of velocity features consistent with the velocities of Roche lobe overflow is unexpected. It appears that J2048 was experiencing an interval of enhanced mass transfer during our observations. We briefly discuss scenarios that might lead to such a situation, such as changes in the chromospheric activity level on the secondary star.

Key words: stars: individual: J204827.9+005008.9 – stars: late-type – stars: magnetic fields – novae, cataclysmic variables.

1 INTRODUCTION

The Hamburg Quasar Survey and Sloan Digital Sky Survey (SDSS) revealed a new group of detached binaries in which a highly magnetized white dwarf (WD) ($B \geq 60$ MG) is tidally and/or magnetically locked to its M dwarf companion in a period of $\leq$4.5 h. The magnetic field of the white dwarf grabs the wind of the M dwarf, directing it on to the magnetic pole(s); this gives rise to cyclotron humps, which are the main spectroscopic identifier of the magnetic nature of the binaries. Because of their low mass transfer rates ($\dot{M} \leq 10^{-13}\,M_\odot\,yr^{-1}$), those systems were dubbed 'low-accretion-rate polars (LARPs; Schwope et al. 2002b), to distinguish them from magnetic cataclysmic variables (polars) in which accretion starts from the L1 point before being threaded on to the magnetic field of the white dwarf and falling to one or both magnetic poles. The accretion rate in LARPs is more than two orders of magnitude smaller than the accretion rate in polars (Schmidt et al. 2005, hereafter S05). Furthermore, their white dwarf temperatures are cooler than the white dwarf temperatures in polars, suggesting an older population and lack of recent accretion history. These two points were sufficient arguments to conclude that LARPs are not likely to represent polars in prolonged low states. Whether they are or not progenitors of polars is still under debate (S05; Webbink & Wickramasinghe 2005). To date, nine such systems (e.g. S05; Schmidt et al. 2007; Schwope et al. 2009) have been discovered, all having strong cyclotron humps in the optical, corresponding to magnetic field strengths between 60 and 70 MG.

The subject of this paper, SDSS J204827.9+005008.9 (hereafter J2048), was first studied by S05 as a new LARP discovered in the SDSS survey. The binary consists of a comparatively cool ($T \lesssim 7500$ K) white dwarf and an M3 dwarf, magnetically locked in a period of 4.2 h. The very low mass transfer rate ($\dot{M} \sim 5 \times 10^{-14}\,M_\odot\,yr^{-1}$) is consistent with accretion solely via the wind from the companion. Cyclotron features and spectropolarimetry determined the magnetic field strength of the white dwarf to be $\sim$62 MG. We obtained 4.3 h of optical spectra of the system, in order to study the structure and origin of its emission spectral features, with rather surprising results.

2 SPECTROSOCPIC OBSERVATIONS

We monitored spectroscopically J2048 using the FOcal Reducer and low dispersion Spectrograph (FORS) on the UT2 8-m telescope of European Southern Observatory (ESO) during one night in 2008 May. We used GRISM 1200R, centred around the Hα line, with a wavelength coverage between 5800 and 7300 Å. This provided a dispersion of $\sim$0.7 Å pixel^{-1} and a resolution of 2.6 Å [full width at half-maximum (FWHM)]. Data processing took place using the

★E-mail: skafka@dtm.ciw.edu
†Present address: Department of Terrestrial Magnetism, Carnegie Institution of Washington, 5241 Broad Branch Road NW, Washington, DC 20015, USA.
‡Present address: Departamento de Fisica y Astrofsica, Universidad de Valparaiso, Av. Gran Bretana 1111, Valparaiso, Chile.

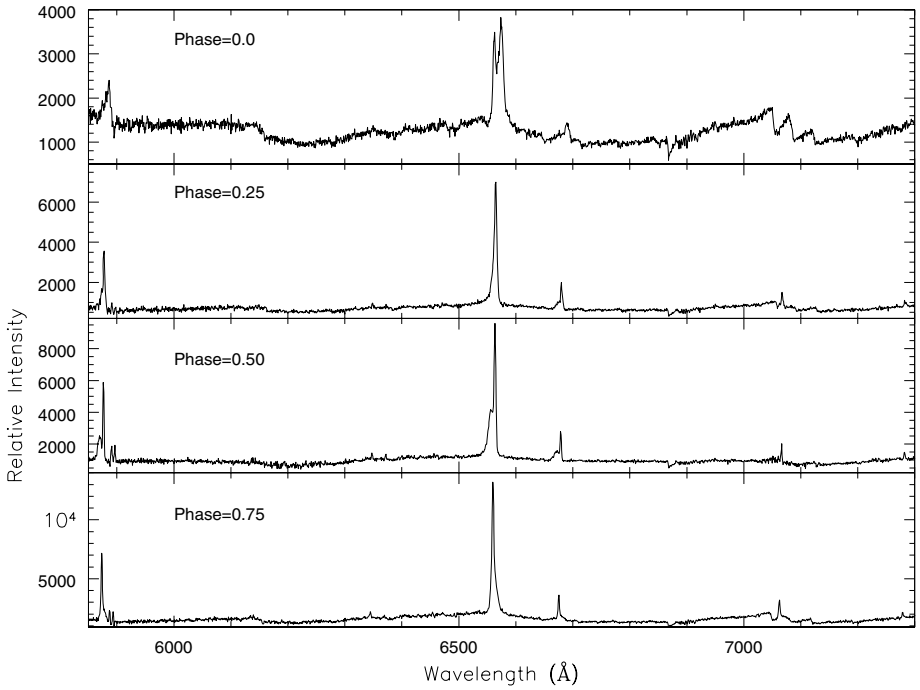

Figure 1. Example spectra at 0.25 phase intervals. Note the profile of the Hα line, which is clearly double peaked at some phases. At phase 0.5, the TiO bands are weaker and the NaD lines are in emission likely due to irradiation on to the inner hemisphere of the M dwarf. The He I emission lines are also seen to have considerable structure.

IRAF[1] packages TWODSPEC and ONEDSPEC. For wavelength calibrations, we used spectra of a HeNeAr lamp, taken at the beginning of the night. Due to unfavourable weather conditions, we were not able to obtain spectrophotometric standards.

The system is 19.4 mag in SLOAN-g filter and its reported orbital period is 4.2 h (S05). As a compromise between the need for a sufficiently high phase resolution in order to keep orbital smearing of important features to a minimum and the need for decent signal-to-noise ratio, we chose an exposure time of 15 min.

We obtained a total of 19 spectra on the target, which corresponds to 4.3 h of observing. Strong winds prevented us from obtaining more than one orbit of the system, therefore we are unable to examine possible orbit-to-orbit variations in the line profiles, although existing photometry reports that no large changes are taking place in successive orbits of the system (S05).

3 ANALYSIS

Fig. 1 shows examples of spectra of J2048 at four different orbital phases. We have assigned phases for our spectra based on the radial velocity (RV) curve of TiO from the secondary star, plus the orbital period of 4.2 h from S05. We measured the TiO band near 7120 Å; the bluer and somewhat stronger TiO band head is disturbed by He I 7065 Å emission. The $-$ to $+$ crossing of the TiO RV curve through the γ velocity (marking inferior conjunction of the secondary star) defines orbital phase zero for this study. Details on this RV curve are found later in this section when discussing the value of K_2. The NaD emission lines disappear near phase zero, indicating that the likely originates on the inner hemisphere of the M star. In all our spectra, the Hα line is in emission, along with He I 5876, 6678 and 7065 Å, although significantly diminished around phase 0.0. In the discovery paper, S05 report that the Balmer emission lines in their spectra are 'very narrow' and that the He II 4686 line is absent. They concluded that the emission is a result of irradiation on to the inner face of the M star alone, and not accretion induced. They also interpret asymmetries in the emission-line profiles to asymmetric irradiation of the M star. Since the X-ray source responsible for the irradiation field is the magnetic pole(s) of the white dwarf, the reported asymmetries suggest that the heating pole is not directly opposite to the inner hemisphere of the M star.

In our data, Hα and all He I emission lines have two components at most phases. This is quite different from the narrow single-peaked lines in the S05 SDSS and Apache Point Observatory (APO) spectra of J2048 taken in 2004, which have spectral and time resolutions similar to our data. No linewidths or strengths are provided in S05, but their SDSS spectra (3.6 Å resolution) are described as having 'prominent narrow Balmer emission lines' while the Balmer lines in the orbit-resolved APO spectra (3 Å resolution) are 'very narrow, ruling out an origin in an infalling stream'. He I emission appears to be absent in the single SDSS spectrum of J2048 shown in S05, whereas it is prominent in our spectra. Finally, their Bok spectra show a narrow Hα line and no He I emission (S05, fig. 6). Even the line profiles in the S05 Bok spectra at 15 Å resolution are inconsistent with our 2008 spectra because, upon degrading our spectra to the Bok resolution, structured line profiles remained easily visible at some phases. It appears that at the times of the S05 spectral data (acquired at three epochs over $\sim$6 weeks in 2004) J2048 had more narrow and less structured line profiles, as well as lower excitation, than our single-epoch spectra in 2008. For future reference, we provide in Table 1 the equivalent widths (EW) and FWHM of the full Hα line in our data, as a function of orbital phase.

[1] IRAF is distributed by the National Optical Astronomy Observatories, which are operated by the Association of Universities for Research in Astronomy, Inc., under cooperative agreement with the National Science Foundation.

Table 1. Full Hα line strengths.

HJD 2445 4616	Phase	EW (Å)	$\mathrm{FWHM_{Voigt}}$
0.72	1.00	−41.18	8.76
0.73	0.06	−52.29	5.16
0.74	0.12	−58.03	5.00
0.75	0.18	−44.15	8.15
0.76	0.24	−64.26	8.06
0.77	0.31	−54.85	4.90
0.78	0.37	−41.19	4.04
0.79	0.43	−37.03	4.17
0.80	0.49	−39.76	3.94
0.82	0.55	−36.47	4.77
0.83	0.62	−38.58	6.65
0.84	0.68	−35.21	12.70
0.85	0.74	−29.46	15.49
0.86	0.80	−26.5	20.98
0.87	0.87	−26.96	19.58
0.88	0.93	−36.41	12.66
0.89	0.99	−49.46	9.99
0.90	0.05	−47.56	7.28
0.91	0.11	−60.58	5.02

Table 2. Parameters of the measured features in J2048.

Line	γ (km s^{-1})	K (km s^{-1})	ϕ_0
Hα (centre)	-27.57 ± 1.27	119.97 ± 8.21	-0.014 ± 0.017
He I 5876 Å	-26.74 ± 0.51	101.10 ± 5.34	-0.012 ± 0.013
NaD (average)	-36.82 ± 1.53	110.39 ± 3.91	0.011 ± 0.007
He I 6678 Å	10.23 ± 1.55	123.82 ± 5.85	0.047 ± 0.009
He I 7065 Å	2.21 ± 6.15	77.08 ± 10.63	-0.020 ± 0.936
TiO 7120 Å	-29.87 ± 3.54	204.57 ± 4.73	0.006 ± 0.004

For our study of orbital RVs, we used only the well-defined central component for all lines. For spectral decomposition, we used Voigt line profile fits, available in the IRAF/SPLOT package. By fitting sinusoids of the form $v(t) = \gamma - K \sin[2\pi(\phi - \phi_0)]$, we derived the systemic velocity (γ), the semi-amplitude velocity of the sinusoidal fit (K) and the zero-phase (ϕ_0) values for each of the emission lines; the values are shown in Table 2. The TiO RV curve was determined by taking the mean of cursor positions at the two inflection points of the band head, yielding $K_{\mathrm{TiO}} = 205 \pm 5\,\mathrm{km\,s^{-1}}$ with an overall $\sigma_{\mathrm{fit}} = 26\,\mathrm{km\,s^{-1}}$. We find that the band is weakened by only approximately two times at superior conjunction. This suggests that the varying TiO strength over the surface of the secondary star may not affect the amplitude of the RV curve to a large extent. Furthermore, both NaD components are in emission for most of the orbit, disappearing between phases 0.7 and 0.95. Since NaD originates on the irradiated M3 star, this indicates non-uniform heating of the inner hemisphere, consistent with the conclusion of S05.

The bottom panel of Fig. 2 shows a Doppler map of the Hα line of the system. For this Doppler map, we used the maximum entropy FORTRAN code of Spruit (1998) within the European Southern Observatory–Munich Image Data Analysis System (ESO–MIDAS) interface. Doppler maps are computed with a smearing kernel of 2 pixels. To place the centre of mass at velocity coordinates (0, 0), the spectra have to be corrected for the centre-of-mass velocity term γ. The γ velocity from the RV fit usually serves as a first guess only, and is iteratively adjusted by comparing the average original spectrum with the one reconstructed from the Doppler map. A review of

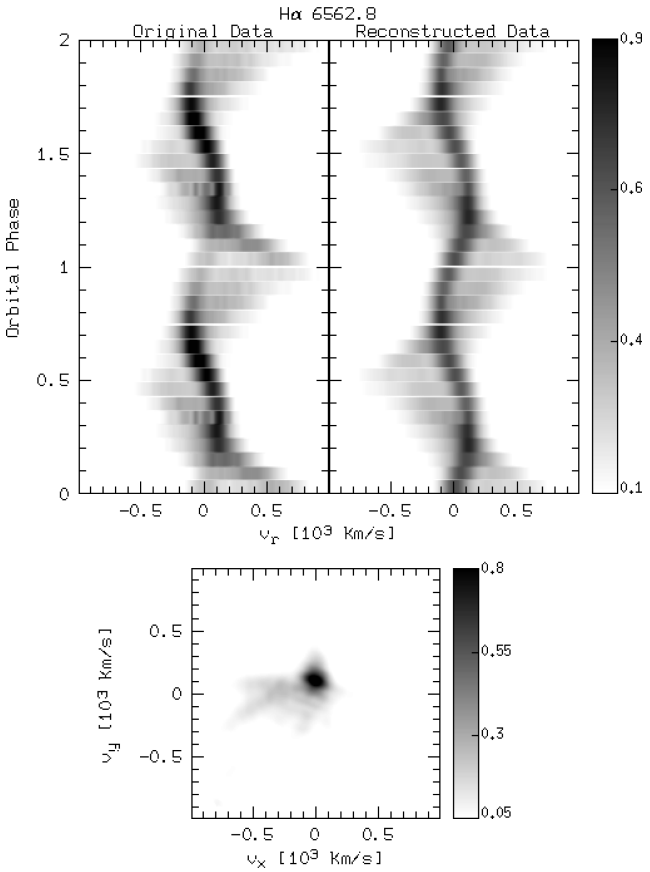

Figure 2. Doppler tomogram of the Hα emission line (bottom panel). The top plots show the original trailed spectrum (left) and the reconstructed one from the Doppler map (right). All plots are normalized to a maximum intensity of 1.0. The intensity cuts of the plots are 0.1 and 0.9 for the trailed spectra and 0.05 and 0.8 for the Doppler map.

magnetic cataclysmic variable (CV) Dopper maps for one- and two-pole accreting magnetic CVs can be found in Schwope et al. (2009); collections of tomograms are abundant in the literature (e.g. Hoard 1999). A consistency check is provided by comparing the trailed spectrum constructed from the data with the one constructed from projections of the derived Doppler map. It is seen in Fig. 2 (top panel) that all the major features in the trailed spectrum are also found in the reconstruction. Note that the intensity variations in the original data especially evident around phase 0.0 and probably due to obscuration are not reproduced, since the Doppler tomography assumes that all emission sources are visible at all phases.

4 DISCUSSION

From the trailed spectra of Fig. 2, it is evident that the Hα line has two main components: a central low-amplitude sinusoid and a larger amplitude satellite. In the Doppler map, we see that the bulk of the emission (the central component) corresponds to the inner hemisphere of the secondary star, likely arising from irradiation. The higher velocity line component in the Hα lines maps into the broad feature in the Doppler map extending towards $-400\,\mathrm{km\,s^{-1}}$, $0\,\mathrm{km\,s^{-1}}$ (for v_x, v_y).

The high-amplitude component of the He I and Hα emission lines is intriguing. The accepted scenario is that, in LARPS, the M star is well within its Roche lobe; therefore, there is no accretion stream (as opposed to magnetic cataclysmic variables). Instead, the white

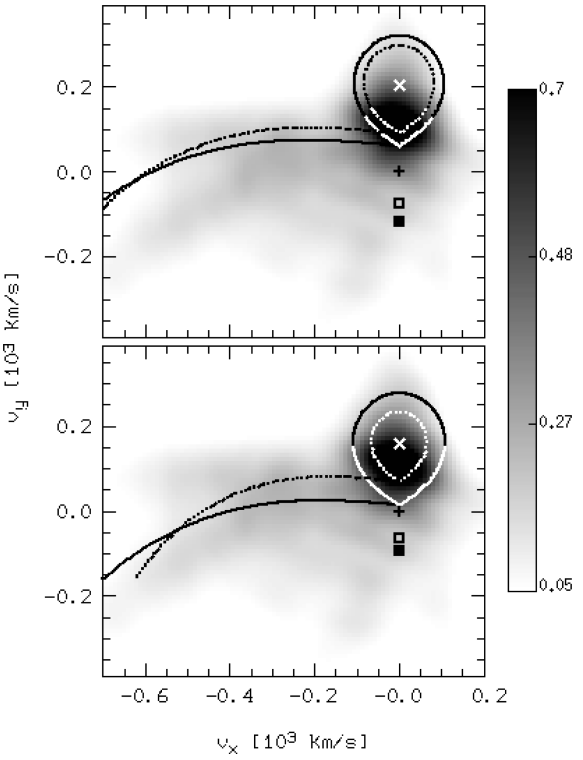

Figure 3. Closeup of the Hα Doppler map. Superimposed are calculations of the ballistic stream and the Roche lobe of the secondary for white dwarf masses of $0.6\,M_\odot$ (solid lines) and $0.9\,M_\odot$ (dotted line). In both plots, symbols mark the positions of K_2 ($\times$), the centre of mass (+) and the K_1 of the two primary masses (solid and open squares for 0.6 and $0.9\,M_\odot$, respectively). The top plot shows the respective streams and lobes assuming that the RV curve of the TiO band tracks the centre of mass of the secondary, i.e. $K_2 = K_{\rm TiO} = 205\,{\rm km\,s^{-1}}$. For the lower plot, an arbitrary $K_2 = 160\,{\rm km\,s^{-1}}$ was used explore a possible irradiation effect in the TiO RVs.

dwarf magnetic field directs almost all the wind of the M star towards the WD magnetic pole(s). Wind accretion is also suggested to be present in polars during the low states, where accretion temporarily drops to a value of $\sim 10^{-12}\,M_\odot\,{\rm yr}^{-1}$ (Hessman, Gänsicke & Mattei 2000). Therefore, low-state polars should resemble LARPs in their accretion characteristics. However, recent spectroscopic observations of low-state polars revealed the presence of high-amplitude components in the Hα line (similar to the ones in J2048). In the case of polars, though, the high-velocity components originated close to the M star, and were interpreted as being due to magnetically controlled gas, streaming along prominence-like structures likely kept in place by interactions of the magnetic dipoles of the two stars (Kafka et al. 2008, and references therein). This kind of Hα structure has now been observed in five magnetic CVs in the low state,[2] making it a characteristic of the group. Doppler maps and trailed spectra of low-state polars do not show any indications of an accretion stream.

In Fig. 3, we show a close-up of the Hα Doppler map, and we overplot the Roche lobe of the secondary and the track of a ballistic stream for several different system parameters. For this, we assumed the mass of the M3 dwarf to be $M_2 = 0.35\,M_\odot$. The mass of the white dwarf is a free parameter; in Fig. 3, we show the results for $M_1 = 0.6\,M_\odot$ (which is the value used by S05) and $M_1 = 0.9\,M_\odot$. From this, we can calculate the non-projected velocities (i.e. corresponding to an inclination $i = 90$). The choice of the projected velocity of the M3 dwarf, K_2, then determines the inclination i and the projected velocity of the primary K_1, i.e. its position on the Doppler map. For our calculations, we used $K_2 = K_{\rm TiO} = 205\,{\rm km\,s^{-1}}$ and an arbitrary, significantly lower, $K_2 = 160\,{\rm km\,s^{-1}}$. The motivation for the latter was to explore the potential influence of irradiation, which in principle could cause the velocities of the TiO band to be higher than that of the centre of mass, i.e. $K_{\rm TiO} > K_2$. The resulting inclinations are (here, we indicate the white dwarf mass as a subscript) $i_{0.6} = 60^\circ, i_{0.9} = 44^\circ$ for $K_2 = K_{\rm TiO}$, and $i_{0.6} = 43^\circ, i_{0.9} = 33^\circ$ for $K_2 = 160\,{\rm km\,s^{-1}}$. We have already remarked in a previous section on the weakened Hα line around inferior conjunction (phase 0.0). The most probable explanation for this is an obscuration of the emission source by the M3 dwarf. This, together with the absence of an eclipse, suggests a medium-high inclination, so $i = 60^\circ$ for $M_1 = 0.6\,M_\odot$ and $K_2 = 205\,{\rm km\,s^{-1}}$ appear to be reasonable values. The other parameter combinations yield $i < 50^\circ$, which seems too low. We note that lower white dwarf masses combined with a low K_2 can also yield medium-high inclinations, e.g. the pair $M_1 = 0.4\,M_\odot$ and $K_2 = 160\,{\rm km\,s^{-1}}$ gives $i = 60^\circ$. Still, a large majority of CVs with periods $P_{\rm orb} < 0.2$ d have mass ratios $q = M_2/M_1 < 0.7$ (Ritter & Kolb 2003, update 2.11). This is therefore another point in favour of the TiO band velocity not being significantly affected by irradiation, and that $K_2 \sim K_{\rm TiO}$.

Regarding the stream calculations for our preferred M_1– K_2 pair, we observe that, although there is some offset, the ballistic stream path matches the location and curvature in velocity space of the high-amplitude line component in Hα. This behaviour is common in accreting polars, but is unexpected in a detached system such as J2048. In synchronously rotating binaries with a highly magnetized white dwarf, the magnetic field of the companion is locked to the magnetic field of the white dwarf, resulting in a complex magnetic configuration described in a series of papers by Li, Wickramasinghe & Wu (1995). The authors investigate the case of polars and explore the efficiency of magnetic braking from the wind of the donor star, for different magnetic field strengths of the white dwarf and orientations of the magnetic axes (for both stellar components). Webbink & Wickramasinghe (2005) conclude that for the B fields found in LARPS it is energetically possible for the white dwarf to capture the entire wind of the red dwarf, a process dubbed a 'magnetic siphon'. S05 argue that, for such a low mass accretion rate, a siphon should be in action in J2048. It is beyond the scope of this paper to model the expected tomographic signature of a siphon in J2048, particularly since the orientation of the magnetic poles of the white dwarf with respect to the orbit is not known. However, if the observed structure in the tomogram represents a siphon, we would expect to also see the magnetic component of the accretion flow (which leads material on to the white dwarf), not the ballistic part of a stream alone.

While a siphon may have contributed to the accretion flow at the time of our observations, the changes in line profiles, plus the appearance of He I emission, plus the consistency of the Hα Doppler map with an accretion stream altogether argue that the accretion mode (and perhaps the accretion rate as well) was different at the time of our observations. Under the assumption that the secondary star in J2048 is well within its Roche lobe, as in other LARPS (Webbink & Wickramasinghe 2005; S05), this leaves stellar activity on the secondary star as the likely culprit (Schwope et al. 2002a). An accretion blob escaping from L1 might result from a strong

[2] AM Her (Kafka et al. 2008), ST LMi (Kafka et al. 2007), VV Pup (Mason et al. 2008), BL Hyi (Kafka et al., in preparation), EF Eri (S. Kafka; results not available yet).

flaring event (Saar, Kashyap & Ringwald 2007), and the rapidly rotating M dwarfs in CVs are expected to be very chromospherically active. We have no reliable way to assess the level of chromospheric activity on the M star at the time of our spectra. However, we note that the Doppler maps in Figs 2 and 3 do show some emission at velocities consistent with the backside of the M dwarf. This emission is approximately 10 times weaker than the emission on the inner hemisphere (which is likely due to irradiation) and may arise from a distribution of active regions over the full surface of the star. As discussed earlier in this section, most low-state polars show evidence for prominence-like structures likely kept in place by interactions of the magnetic fields of the two stars. We find it puzzling that such features are not seen in J2048, especially in light of other arguments for activity on the secondary star. A possible explanation is that the star is saturated with small-scale activity regions (Mohanty & Basri 2003; Reiners, Basri & Browning 2009) capable of Hα emission but which inhibit large-scale magnetic connections between the two stars.

5 CONCLUSIONS

Assuming $M_2 = 0.35\,\mathrm{M}_\odot$, our measurement of $K_2 = K_{\mathrm{TiO}} = 205\,\mathrm{km\,s^{-1}}$ leads to $i \sim 60^\circ$, $M_1 \sim 0.60\,\mathrm{M}_\odot$ and $q = M_2/M_1 \sim 0.58$. These parameters, along with Doppler mapping, are used to help interpret the considerable structure we find in the emission-line profiles of J2048. These features differ from those seen in previous epochs of spectroscopic observations, and suggest that J2048 was undergoing an accretion episode at the time of our observations. Although J2048 is very similar to a low-state polar in that it consists of a fast-rotating M star and a highly magnetic white dwarf, its Doppler map indicates that the high-velocity emission line component differs from that in low-state polars. In low-state polars, the high-velocity components of the Hα line has been attributed to gas flowing along large-scale prominences near the secondary star, consistent with the expected strong chromospheric activity in the rapidly rotating M dwarfs component of the system. In J2048, the high-velocity component originates from a feature that is quite near to the velocities expected from an L1 accretion stream. This is a puzzle because in J2048 mass transfer is expected to take place via a wind from the secondary, not via L1.

ACKNOWLEDGMENTS

We would like to thank Don Hoard for fruitful discussions.

REFERENCES

Hessman F. V., Gänsicke B. T., Mattei J. A., 2000, A&A, 361, 952
Hilton E. J., Szkody P., Mukadam A., Henden A., Dillon W., Schmidt G. D., 2009, AJ, 137, 3606
Hoard D. W., 1999, in Hellier C. & Mukai K., eds, ASP Conf. Ser. Vol. 157, Annapolis Workshop on Magnetic Cataclysmic Variables. Astron. Soc. Pac., San Francisco, p. 201
Kafka S., Howell S. B., Honeycutt R. K., Robertson J. W., 2007, AJ, 133, 1645
Kafka S., Ribeiro T., Baptista R., Honeycutt R. K., Robertson J. W., 2008, ApJ, 688, 1302
Li J., Wickramasinghe D. T., Wu K., 1995, MNRAS, 276, 255
Mason E., Howell S. B., Barman T., Szkody P., Wickramasinghe D., 2008, A&A, 490, 279
Mohanty S., Basri G., 2003, ApJ, 583, 451
Reiners A., Basri G., Browning M., 2009, ApJ, 692, 538
Ritter H., Kolb U., 2003, A&A, 404, 301, update 2.11 (Jan 2009)
Saar S. H., Kashyap V. L., Ringwald F. A., 2007, in Gómez de Castro A. I., Barstow M. A., eds, Proc. Joint Discussion n. 4 during the IAU General Assembly of 2006, UV Astronomy: Stars from Birth to Death. WSO-UV, Madrid, p. 249
Schmidt G. D. et al., 2005, ApJ, 630, 1037 (S05)
Schmidt G. D., Szkody P., Henden A., Anderson S. F., Lamb D. Q., Margon B., Schneider D. P., 2007, ApJ, 654, 521
Schwope A. D., Brunner H., Hambaryan V., Schwarz R., 2002a, in Gänsicke B. T., Beuermann K., Reinsch K., eds, ASP Conf. Ser. Vol. 261, The Physics of Cataclysmic Variables and Related Objects. Astron. Soc. Pac., San Francisco, p. 102
Schwope A. D., Nebot Gomez-Moran A., Schreiber M. R., Gaensicke B. T., 2009, A&A, 500, 867
Spruit H. C., 1998, preprint (astro-ph/9806141)
Webbink R. F., Wickramasinghe D. T., 2005, in Hameury J.-M., Lasota J.-P., eds, ASP Conf. Ser. Vol. 330, The Astrophysics of Cataclysmic Variables and Related Objects. Astron. Soc. Pac., San Francisco, p. 137

This paper has been typeset from a TEX/LATEX file prepared by the author.